Wang *et al. Journal of Ovarian Research* (2025) 18:25
https://doi.org/10.1186/s13048-025-01608-3

Journal of Ovarian Research

RESEARCH Open Access

Dynamic and functional analyses of exosomal miRNAs regulating cellular microenvironment of ovarian cancer cells

Zhaoxia Wang[1,3*], Yanan Huang[1], Simin He[2], Ying Zhou[1], Le Zhao[1] and Fuyuan Wang[1]

Abstract

Background Exosomes, extracellular vesicles with an average diameter of 30 ~ 150 nm, are pivotal in mediating the cellular microenvironment (CM) through their cargo-carrying capability. Despite extensive studies, the dynamic and regulatory mechanisms of exosomal cargoes, including lipids, proteins, nucleic acids, and metabolites, remain poorly understood.

Methods In this study, we collected culture medium of ovarian cancer cells at four different time points (12, 24, 36, 48 h). Exosomes were isolated using ultracentrifugation, and miRNA sequencing was performed for exosomes from each group (T12, T24, T36, and T48).

Results A total of 131 miRNAs were identified in all groups. Specifically, 41, 115, 63, and 24 miRNAs were detected in the T12, T24, T36, and T48 groups, respectively. Among these, 15 miRNAs were common to the all groups, while 3, 57, 10, and 3 miRNAs were unique to the T12, T24, T36, and T48 groups, respectively. Functional analyses of the target genes for both common and specific miRNAs indicated that numerous target genes were involved in signaling pathways and cancer-related processes.

Conclusion It suggested that exosomal miRNAs might be critical in intercellular communication and in dynamically remodeling the tumor microenvironment. These insights could enhance our understanding of the role of exosomal miRNAs in cancer biology and inform the development of novel therapeutic strategies.

Keywords Cellular microenvironment, Ovarian cancer, Exsomes, miRNAs, miRNA sequencing

Introduction

Cellular microenvironment (CM), which consists of spatiotemporal gradients of multiple physical and chemical cues, plays an essential role in mediating cell behaviors including spreading, proliferation, apoptosis, differentiation and migration, especially for pathological processes such as tumor formation and progression [1]. Exosomes, secreted by all cell types in organisms from bacteria to humans and plants, are lipid bilayer vesicles with an average diameter of 30 ~ 150 nanometers [2, 3]. Multiple studies indicated that exosomes might play important roles in remodeling CM [4, 5]. Once secreted, exosomes

*Correspondence:
Zhaoxia Wang
wzx35181196@126.com
[1]Department of Gynecology, First Hospital of Shanxi Medical University, Taiyuan, Shanxi, People's Republic of China
[2]Department of Health Statistics and Epidemiology, School of Public Health, Shanxi Medical University, Taiyuan, Shanxi, People's Republic of China
[3]First Hospital of Shanxi Medical University, 85 South Jiefang Road, Taiyuan, Shanxi 030001, P.R. China

cruise through the local CM, or are delivered through circulating body fluids to distal organs, where they interact with or enter target cells to induce cell phenotypic changes [6, 7].

There are multiple biomolecules exist in exosomes, such as lipids, proteins, nucleic acids and metabolites [8]. MicroRNAs (miRNAs), a type of regulatory non-coding RNA, are often sorted into exosomes by complicated mechanism, and promote paracrine and endocrine communication between different tissues, which regulate gene expression, and remotely control cellular processes.

Hence, the potential role and mechanism of miRNAs from exosomes in the prevention, diagnosis and treatment of different types of diseases have attracted the attention of thousands of researchers [9]. However, how the exosomal miRNAs or other biomolecules regulate the CM is still kept elusive.

In the current study, we tried to explore the dynamic and molecular mechanism of exsomal miRNAs regulating CM of ovarian cancer (OC) cells. Therefore, we collected the culture medium of OC cells (SKOV3) at four time points (12, 24, 36 and 48 h), and the exosomes were isolated successfully by a series of centrifugation and ultracentrifugation. The miRNA sequencing (miRNA-seq) was performed for the exosomes samples from the different groups (T12, T24, T36 and T48), and the bioinformatics analyses and other experiments were carried out.

Method and materials

Cell line and cell culture

Human cell line (SKOV3, RRID: CVCL_0532) was obtained from the Cell Bank of the Chinese Academy of Sciences (Shanghai, China). The cells were cultured in RPMI 1640 medium (Procell, Wuhan, China) supplemented with 10% newborn calf serum (Solarbio, Peking, China) at 37 °C and 5% CO_2. In all experiments, cells were cultured to 80–90% confluence. When the cell confluence was about 70%, the original serum-containing medium was removed and replaced with fresh exosome-free serum medium. The cell culture medium was collected at different time points (12, 24, 36 and 48 h) for subsequent experiments.

Isolation and identification of exosomes

Cell culture medium (50 ml) were centrifuged at 2,500 g for 15 min at 4 °C, and ultracentrifuged at 120,000 g for 2 h to collect exosome pellets. Then, the exosome pellets were washed in filtered 1×PBS (phosphate buffer saline) and re-centrifuged at 120,000 g at 4 °C. Finally, supernatants were discarded, and the pellets were re-suspended in 150 µl 1×PBS.

About 20 µl exosomes were overloaded onto a formvar/carbon-coated grid for 3–5 min. Then we use a filter paper to absorb the excess solution from the edge, and take it to the filter paper to stay about 10 min. After support film was dried, a drop of uranyl acetate dye solution was dripped and dyed for 90 s. Exosomes were then examined with a transmission electron microscopy (TEM) (Hitachi, Japan), which indicated their spherical or disk shape.

The solution containing particles was analyzed using a NanoSight LM20 instrument equipped with a 640 nm laser (NanoSight, Amesbury, UK) at room temperature. The movement of particles was tracked with a NTA (nanoparticle tracking analysis) software (version2.2, NanoSight) with low refractive index corresponding to cell-derived vesicles. The mode, mean, median particle size, and the particle concentration (in millions) for each size was analyzed in each track.

Nano-flow cytometry fluorescence detection

We diluted 30 µl exosomes into 90 µl, and added 20 µl of FITC mouse antibodies (CD9, GeneTex Cat# GTX23923, RRID: AB_385140, CD63, Creative Diagnostics Cat# CABT-33202MH, RRID: AB_2354453 and CD81, Enzo Life Sciences Cat# H00000975-M01, RRID: AB_1504908) (BD Bioscience, CA, USA) to each 30 µl diluted sample. Then, these samples were mixed well and incubated at 37 °C in the dark for 30 min. After 1 ml pre-chilled 1×PBS was added into each sample, these samples were centrifuged at 4 °C, 110,000 × g for 70 min for removing the supernatants; the obtained pellets were re-suspended in 50 µl 1×PBS. Finally, the standard samples as well as the test samples were analyzed using a flow cytometer (NanoFCM, N30E, China) to obtain results of protein markers.

RNA extraction

Total RNAs were extracted from exosomes by using TRIzol (Solarbio, Peking, China), and purified by using two phenol-chloroform treatments. Subsequently, these samples were treated with RQ1 DNase (Promega, Madison, WI, USA) to remove DNAs. The quality and quantity of the purified RNAs was measured by Smartspec Plus (BioRad, Hercules, CA, USA). The integrity of RNAs was further detected by 1.5% agarose gel electrophoresis.

miRNA-seq

Total RNAs (3 µg) from each sample were used to generate small RNA cDNA library with a Balancer NGS Library Preparation kit (Gnomegen, San Diego, CA, USA), according to the manufacturer's protocol. The whole library was submitted to 10% native polyacrylamide gel electrophoresis, and then the bands corresponding to miRNA insertion were cut and eluted. The purified libraries were quantified using the QubitFluorometer (Invitrogen, Thermo Fisher Scientific, Inc.) post

ethanol precipitation and washing. These small RNA libraries were applied to 150 bp pair-end sequencing on the HiSeq 2500 platform (Illumina, Inc., San Diego, CA, USA).

The FASTX-Toolkit (version 0.0.13) (http://hannonlab.cshl.edu/fastx_toolkit/) was used to process raw reads and obtain reliable clean reads. RNAs < 16 or > 30 nts in length were also discarded from next analysis. The clean reads were searched against the Rfam database (version 12.0) using Bowtie [10], and these matches to ribosomal RNAs and transfer RNAs were removed. Hereafter, the remained unique sequences were aligned by using Bowtie against the miRBase database [11], with one mismatch allowed. The aligned small RNA sequences were assured by conserved miRNAs.

To explore the expression profiles of identified miRNAs, the frequency of miRNA counts were normalized to transcripts per million (TPM) with a formula: Normalized expression = actual read count/ total read count $\times 10^6$. The human miRNAs and transcript sequences of miRBase were calculated by miRanda algorithm [12], and the TargetScan was used for predicting putative miRNA targets [13]. To explore the gene function and frequency distribution of functional categories, Gene Ontology (GO) and Kyoto Encyclopedia of Genes and Genomes (KEGG) analyses were conducted using the DAVID bioinformatics database [14].

Quantitative real-time polymerase chain reaction (qPCR)

The qPCR experiment was carried out for detecting expression levels of miRNAs. Some primers were designed for reverse transcription (RT) and qPCR. The primer sequences were as follows: let-7d-5p: 5'- CTC AAC TGG TGT CGT GGA GTC GGC AAT TCA GTT GAG AAC TAT GC -3' (RT), 5'-ACA CTC CAG CTG GGA GAG GTA GTA GGT TGC-3' (forward), 5'-TGG TGT CGT GGA GTC G-3' (reverse); miR-16-5p: 5'-CTC AAC TGG TGT CGT GGA GTC GGC AAT TCA GTT GAG CGC CAA TA-3' (RT), 5'-ACA CTC CAG CTG GGT AGC AGC ACG TAA AT-3' (forward), 5'-TGG TGT CGT GGA GTC G-3' (reverse); U6: 5'-CTC GCT TCG GCA GCA CA-3' (forward), 5'-AAC GCT TCA CGA ATT GTG CGT-3' (reverse).

The cDNAs were produced by standard procedures and real-time PCR was conducted on the Bio-Rad S1000 (BioRad, Hercules, CA, USA) with Bestar SYBR Green RT-PCR Master Mix (DBI Bioscience, Shanghai, China). The PCR conditions consist of denaturing at 95 °C for 8 min, 35 cycles of denaturing at 95°C for 15 s, annealing, and extension at 60°C for 1 min. The qPCR amplifications were performed in triplicates for each sample. Transcript levels for the miRNAs were assessed in comparison with the housekeeping gene U6 as an internal reference standard, using the $2^{-\Delta\Delta CT}$ method [15].

Dual luciferase reporter assay

The sequences of 3' untranslated region UTR of *DEC2* (differentially expressed in chondrocytes protein 2), which contained the wild type (Wt) or mutant (Mut) binding site of hsa-miR-320-3p, were devised and synthesized (Genecreate, Shanghai, China). The synthetic *DEC2* 3' UTR fragment was cloned into pMIR-reporter (Huayuyang, Beijing, China) by endonuclease Spe I and Hind III in order to design complementary mutation sites of seed sequence on DEC2 wild type (Wt). After restriction endonuclease digestion, the target fragment was inserted into the pMIR-reporter plasmid with T4 DNA ligase. The correctly sequenced luciferase reporter plasmids wt and mutant type (mut) were co-transfected with miR-320-3p into HEK-293T cells (Xinyu, Shanghai, China). After 48 h of transfection, the cells were harvested and lysed. A luciferase assay kit (Beyotime, Shanghai, China) as well as a Glomax20/20 luminometer fluorescence detector (Promega, Madison, WI, USA) was employed to detect luciferase activity. The relationship between DEC2 and miR-320-3p was detected using the same method. The experiment was repeated five times in each group.

Protein extraction and Western blot

The ovarian cells were treated on ice for 30 min with Radio Immunoprecipitation Assay (RIPA) lysis buffer (R0100, Solarbio, Beijing, China) containing protease inhibitors, and then centrifuged for 20 min at 4 ℃and 12,000 RPM. After collecting the supernatant, the protein content was measured using the BCA Protein Assay Kit (CWBIO), and it was denatured by boiling it for ten minutes at 100 ℃. 10% SDS-PAGE was used to separate the denatured proteins, which were then electrophoresed, transferred to PVDF membranes, and blocked for two hours in PBST (phosphate buffered saline, or PBS, with 0.1% Tween-20) containing 5% skim milk powder. Primary rabbit monoclonal antibodies, such as CLOCK, were then used to incubate the blots (Proteintech Cat# 18094-1-AP, RRID: AB_2878497)(1:1000 dilution), BMAL1 (Cat# DF10308, RRID: AB_2840886, Affinity Biosciences)(1:800 dilution), PER2 (ABclonal Cat# A5107, RRID: AB_2863447)(1:800 dilution), CRY1 (RRID: AB_10697652; Proteintech Cat# 13474-1-AP) (1:2000 dilution) HRP-conjugated Affinipure goat anti-mouse IgG (H + L) (1:5000 dilution) or goat anti-rabbit IgG (H + L) (1:500 dilution) for two hours at room temperature after overnight incubation at 4 ℃(1:2000 dilution). GAPDH (RRID: AB_2107436, Proteintech Cat# 60004-1-Ig) A loading control expression of 1:10000 dilution was employed. The blots were then subjected to enhanced chemiluminescence, and the chemiluminescence of the protein bands was measured using a Tanon-5500 Chemiluminescence Imaging System. Image

J software was used to quantify the intensity of certain bands.

Statistical analyses

The data were analyzed for statistical significance with Microsoft Excel (2012), and presented as the mean ± standard deviation (mean ± SD). Student's t-test (paired) was used to assess the statistical significance while comparing the means of two data sets. $P \leq 0.05$ was considered significant, and the false discovery rate (FDR) was applied in some cases.

Online data deposition

The datasets generated in the current study were deposited in the National Center for Biotechnology Information (NCBI) under the accession number PRJNA1108066.

Results

Isolation and characterization of exosomes

When OC cells passage was stable with good viability and consistent growth status, the experiment was performed. The cell culture medium were collected at different times (12, 24, 36 and 48 h). These samples of exosomes were obtained by a series of differential centrifugation, ultracentrifugation, and filtration steps. The extraction procedure and brief protocol was shown in Fig. 1A.

The examination with a TEM indicated that exosomes from four groups showed characteristic round- or cup-shaped morphology and dimension (Fig. 1B). The NTA indicated that average sizes of exosomes from the different time pionts (12, 24, 36 and 48 h) were 122.3, 139.8, 131.8 and 134.9 nm, respectively (Fig. 1C). Moreover, it was found that the number of exosomes per million of cells at the each time point (12, 24, 36, and 48 h) were 8.2×10^8, 2.3×10^{10}, 1.5×10^8 and 4×10^{10}, respectively, showing the obvious differences in the rate of secreting exosomes.

Furthermore, exosomes were validated by nanoflow fluorescence detection indicating the markers (CD9, CD63 and CD81) of exosomes (Fig. 1D), which based on the positive expression results of different antibodies on the exosomes surface. All these results indicated that exosomes were isolated successfully and suitable for further investigation.

Identification of exosomal miRNAs

Previous studies indicated that exosomal miRNAs play important roles in remodeling CM [16, 17], so we tried to investigate the miRNAs cargo of exosomes from the four groups. A total of 12 small RNA libraries (T12-a, T12-b, T12-c; T24-a, T24-b, T24-c; T36-a, T36-b, T36-c; T48-a, T48-b, T48-c) were constructed for miRNA-seq with three biological replicates for each group.

Using Illumina HiSeq 2500, > 298.1 million reads were produced, corresponding to ~ 24.8 million sequence reads per library, and the clean reads account for ~ 95.6%. Hierarchical clustering heatmap analyses revealed that the global expression pattern of miRNAs differed obviously among different groups (Fig. 2A).

Subsequently, these clean reads were matched to Rfam and human reference genome (Ensembl release 102 GRCh38), and the filtered reads were mapped to miRBase. The read counts were normalized to TPM and 131 miRNAs were identified successfully in all samples (Supplementary Table S1). Moreover, 41, 115, 63 and 24 miRNAs were found in T12, T24, T36 and T48 samples respectively, accounting for 31.3%, 87.8%, 48.1% and 18.3% of the all miRNAs identified (Fig. 2B).

RT-qPCR validation

To verify the miRNA-seq results two miRNAs (let-7d-5p and miR-16-5p) were randomly selected from these identified miRNAs and analyzed by RT-qPCR. It showed that the RT-qPCR expression results were highly correlated with miRNA-seq results (Fig. 2C, D). Therefore, the miRNA-seq data were reliable and suitable for further analysis.

Functional analyses of target genes of common exosomal miRNAs

Interestingly, only 15 overlapped miRNAs were found in four groups, including let-7c-5p, let-7a-5p, let-7b-5p, let-7f-5p, let-7i-5p, let-7 g-5p, let-7e-5p, miR-122-5p, miR-1246, miR-16-5p, miR-155-5p, miR-423-5p, miR-1290, miR-3960 and miR-181b-5p, and accounted for 11.4% of the all miRNAs identified.

Generally, the miRNAs could regulate the gene expression by binding to complementary target sites in the mRNAs of their target genes. Using the miRanda algorithm on human miRNA and transcript sequences of miRBase and TargetScan, 398 target genes were found, suggesting that the overlapped miRNAs have the capacity to regulate the expression levels of multiple genes.

To identify the pathways associated with these target genes, GO enrichment analysis was conducted, and 94 biological pathways were identified ($P < 0.01$, FDR < 0.05) (Fig. 3A; Supplementary Table S2). It was found that a large number of enriched terms were associated with signaling, kinase and cell proliferation, including "positive regulation of TOR signaling" (GO:0032008), "positive regulation of Wnt signaling pathway" (GO:0030177), "cell-cell signaling by Wnt" (GO:0198738), "positive regulation of kinase activity" (GO:0033674), "positive regulation of protein kinase activity" (GO:0045860), "regulation of protein serine/threonine kinase activity" (GO:0071900), "positive regulation of protein serine/threonine kinase activity" (GO:0071902), "positive

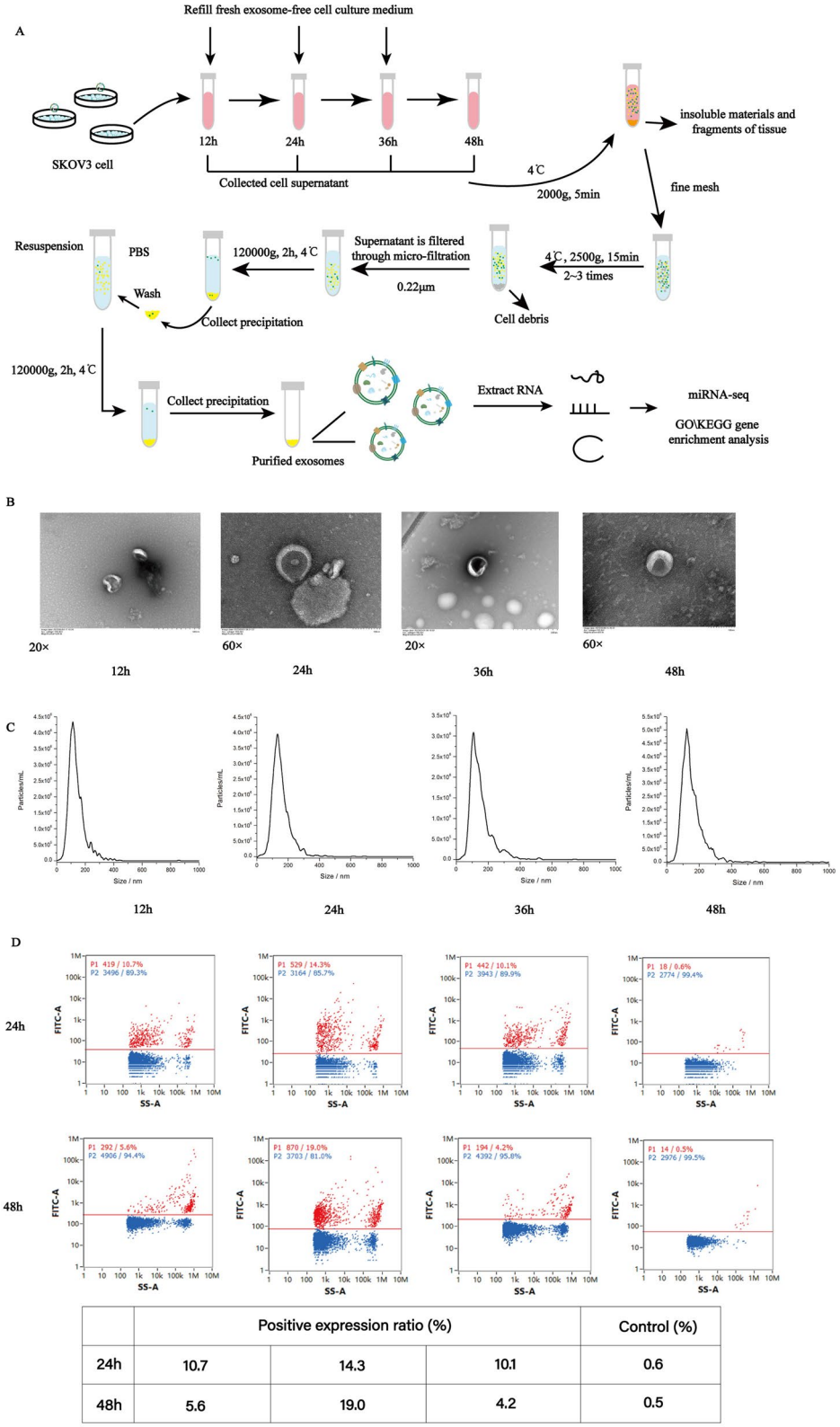

	Positive expression ratio (%)			Control (%)
24h	10.7	14.3	10.1	0.6
48h	5.6	19.0	4.2	0.5

Fig. 1 Characterization of exosomes from ovarian cancer cells at different culture time points. (**A**) A schematic diagram illustrating the experimental design from sample collection till sequencing. (**B**) TEM image of the exosomes. Electron microscopy allowed visualizing membrane-bound nano vesicles sized ~ 100 nm. Scale bar = 100 nm. (**C**) Analysis of exosomes with NanoSight LM10-HS instrument. (**D**) Exosome validation by nanoflow fluorescence indicating the CD9, CD63 and CD81 protein markers for exosomes

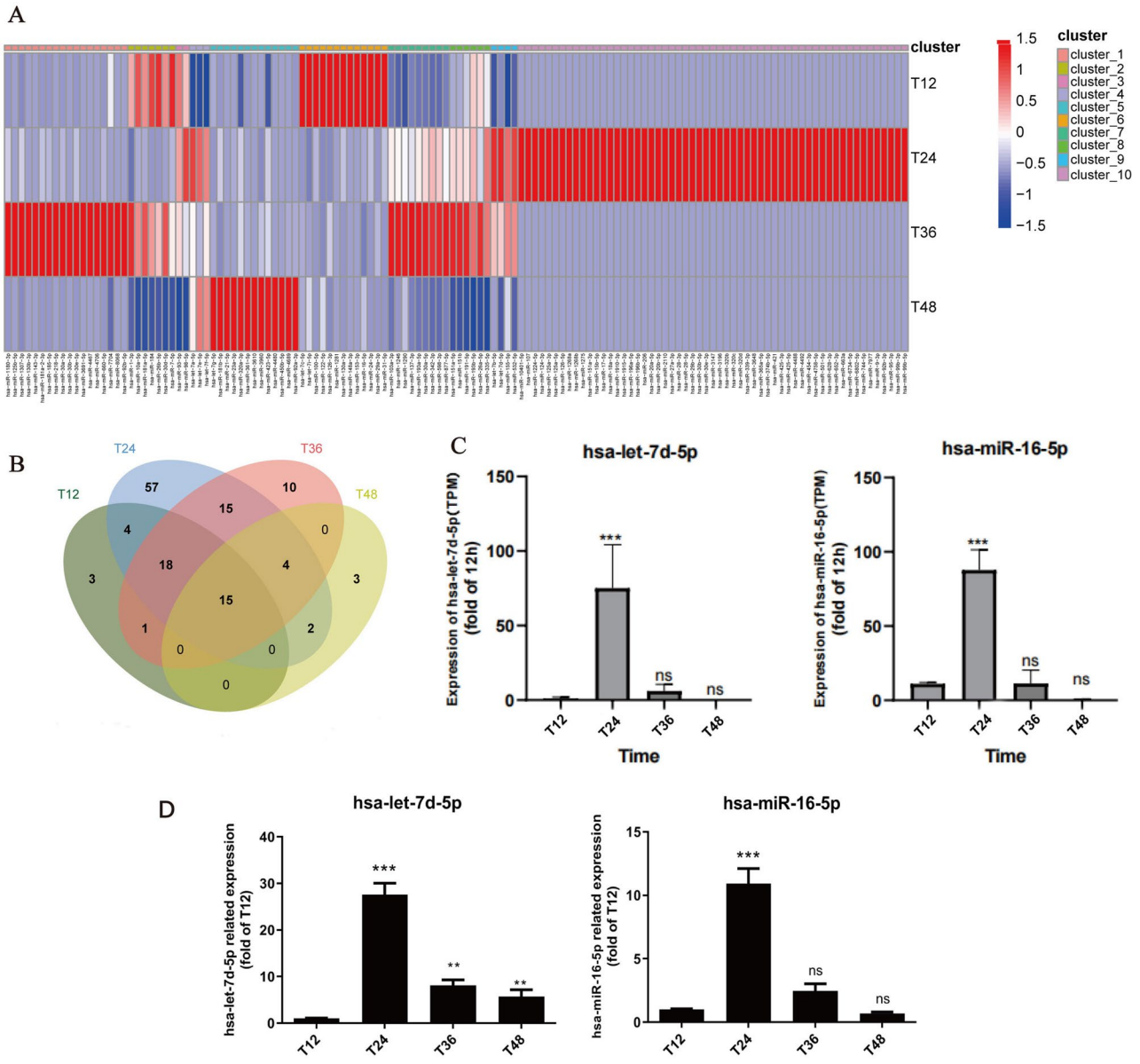

Fig. 2 Identification of exosomal miRNAs by miRNA sequencing. (**A**) Hierarchical clustering heatmap analysis for expression pattern of miRNAs from the four (T12, T24, T36 and T48) groups. (**B**) Venn diagrams of the identified miRNAs from the four (T12, T24, T36 and T48) groups. (**C**) The miRNA expression were determined by high-throughput sequencing. Transcripts per million (TPM) per million mapped reads was used to calculate the expression levels of miRNAs. (**D**) The miRNA expression levels of target genes were determined by RT-qPCR and normalized against U6 expression level. Statistical analysis was performed by Student's t-test and data are presented at the mean ± standard deviation of three replicates. *$P < 0.05$, **$P < 0.01$. RT-qPCR, reverse transcription quantitative real-time polymerase chain reaction

regulation of cell growth" (GO:0030307), "mitotic cell cycle phase transition" (GO:0044772), "regulation of cell growth" (GO:0001558) and "cell growth" (GO:0016049).

In addition, KEGG enrichment analysis was performed for these target genes, and 21 functional terms were obtained ($P < 0.01$, FDR < 0.05) (Fig. 3B; Supplementary Table S3). It indicated that multiple enriched terms were associated with signaling and cancer, including "mTOR signaling pathway" (ID: hsa04150), "IL-17 signaling pathway" (ID: hsa04657), "TNF signaling pathway" (ID: hsa04668), "Signaling pathways regulating pluripotency of stem cells" (ID: hsa04550), "AGE-RAGE signaling pathway in diabetic complications" (ID: hsa04933), "PI3K-Akt signaling pathway" (ID: hsa04151), "MAPK signaling pathway" (ID: hsa04010), "Breast cancer" (ID: hsa05224), "Gastric cancer" (ID: hsa05226), "MicroRNAs in cancer" (ID: hsa05206), "Acute myeloid leukemia" (ID: hsa05221). The results of GO and KEGG analyses suggesting that exosomal miRNAs of OC play important roles in regulating signaling and cancer development.

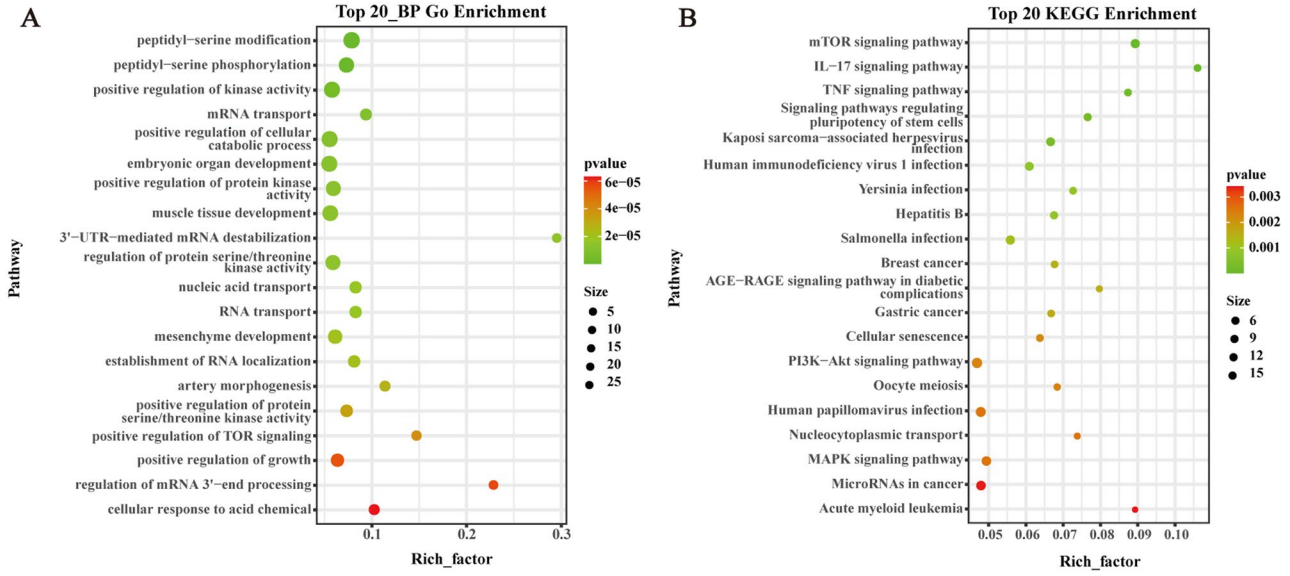

Fig. 3 Functional analyses for the target gene of common miRNAs. (**A**) and (**B**) GO and KEGG analyses for target genes of overlapped miRNA in T12, T24, T36 and T48 groups. miRNA, microRNA; GO, Gene Ontology; KEGG, Kyoto Encyclopedia of Genes and Genomes. The rich factor reveals the enrichment degree of terms, while vertical axis indicates the names of the enriched terms. The area of the node shows the number of genes, while the *p*-value is demonstrated by a color scale with the statistical significance increasing from green to red

Table 1 The specific exosomal miRNAs in four groups

Different time points	miRNA_Name
T12	miR-153-3p, miR-1281 and miR-148a-3p
T24	hsa-miR-95-3p, hsa-miR-320b, hsa-miR-663a, hsa-miR-1268a, hsa-miR-1268b, hsa-miR-744-5p, hsa-miR-320c, hsa-miR-4488, hsa-miR-125a-3p, hsa-miR-4492, hsa-miR-2110, hsa-miR-628-3p, hsa-miR-15b-5p, hsa-miR-20a-5p, hsa-miR-99b-3p, hsa-miR-151a-3p, hsa-miR-3648, hsa-miR-421, hsa-miR-9-3p, hsa-miR-125a-5p, hsa-miR-126-5p, hsa-miR-196a-5p, hsa-miR-6734-5p, hsa-miR-92b-3p, hsa-miR-1915-3p, hsa-miR-320d, hsa-miR-374b-5p, hsa-miR-425-3p, hsa-miR-4758-5p, hsa-miR-501-5p, hsa-miR-10401-5p, hsa-miR-18a-5p, hsa-miR-27a-3p, hsa-miR-28-3p, hsa-miR-28-5p, hsa-miR-30e-3p, hsa-miR-339-3p, hsa-miR-365a-5p, hsa-miR-124-3p, hsa-miR-17-5p, hsa-miR-196b-5p, hsa-miR-20b-5p, hsa-miR-30b-5p, hsa-miR-3196, hsa-miR-6802-5p, hsa-miR-107, hsa-miR-1224-5p, hsa-miR-1275, hsa-miR-1910-3p, hsa-miR-206, hsa-miR-29b-3p, hsa-miR-3147, hsa-miR-425-5p, hsa-miR-454-3p, hsa-miR-652-3p, hsa-miR-7977, hsa-miR-99b-5p
T36	hsa-miR-8068, hsa-miR-92b-5p, hsa-miR-130b-3p, hsa-miR-143-3p, hsa-miR-218-5p, hsa-miR-125b-5p, hsa-miR-30b-3p, hsa-miR-3691-5p, hsa-miR-4467, hsa-miR-4706,
T48	hsa-miR-3610, hsa-miR-4480, hsa-miR-450b-5p

Functional analyses of target genes of specific exosomal miRNAs

It indicated that 3, 57, 10 and 3 specific miRNAs were also found in T12, T24, T36 and T48 groups (Fig. 2B; Table 1), respectively.

There were 199 putative target genes of the specific miRNAs in T12 group, and the KEGG analyses were performed. The results indicated that 34 terms were enriched ($P < 0.05$, FDR < 0.65) (Fig. 4A; Supplementary Table S4), and the most of terms were associated with cancer and signaling, including "FoxO signaling pathway" (ID: hsa04068), "Colorectal cancer" (ID: hsa05210), Hepatocellular carcinoma" (ID: hsa05225), "Breast cancer" (ID: hsa05224), "MAPK signaling pathway" (ID: hsa04010), "PI3K-Akt signaling pathway" (ID: hsa04151), "Proteoglycans in cancer" (ID: hsa05205), "Signaling pathways regulating pluripotency of stem cells" (ID: hsa04550), "Gastric cancer" (ID: hsa05226), "Basal cell carcinoma" (ID: hsa05217) and "TGF-beta signaling pathway" (ID: hsa04350), "Non-small cell lung cancer"(hsa05223), "Pancreatic cancer"(hsa05212), "Ras signaling pathway"(hsa04014), "ErbB signaling pathway"(hsa04012),"Micro-RNAs in cancer"(hsa05206), "Estrogen signaling pathway"(hsa04915) "GnRH signaling pathway"(hsa04912), "mTOR signaling pathway"(hsa04150), "Hippo signaling pathway"(hsa04390) and "Endometrial cancer"(hsa05213).

There were 1601 putative target genes of the specific miRNAs in T24 group, and the KEGG analyses indicated that 92 terms were enriched ($P < 0.05$, FDR < 0.65) (Fig. 4B; Supplementary Table S5). It was found that the most of terms were associated with cancer and signaling, including "MAPK signaling pathway"

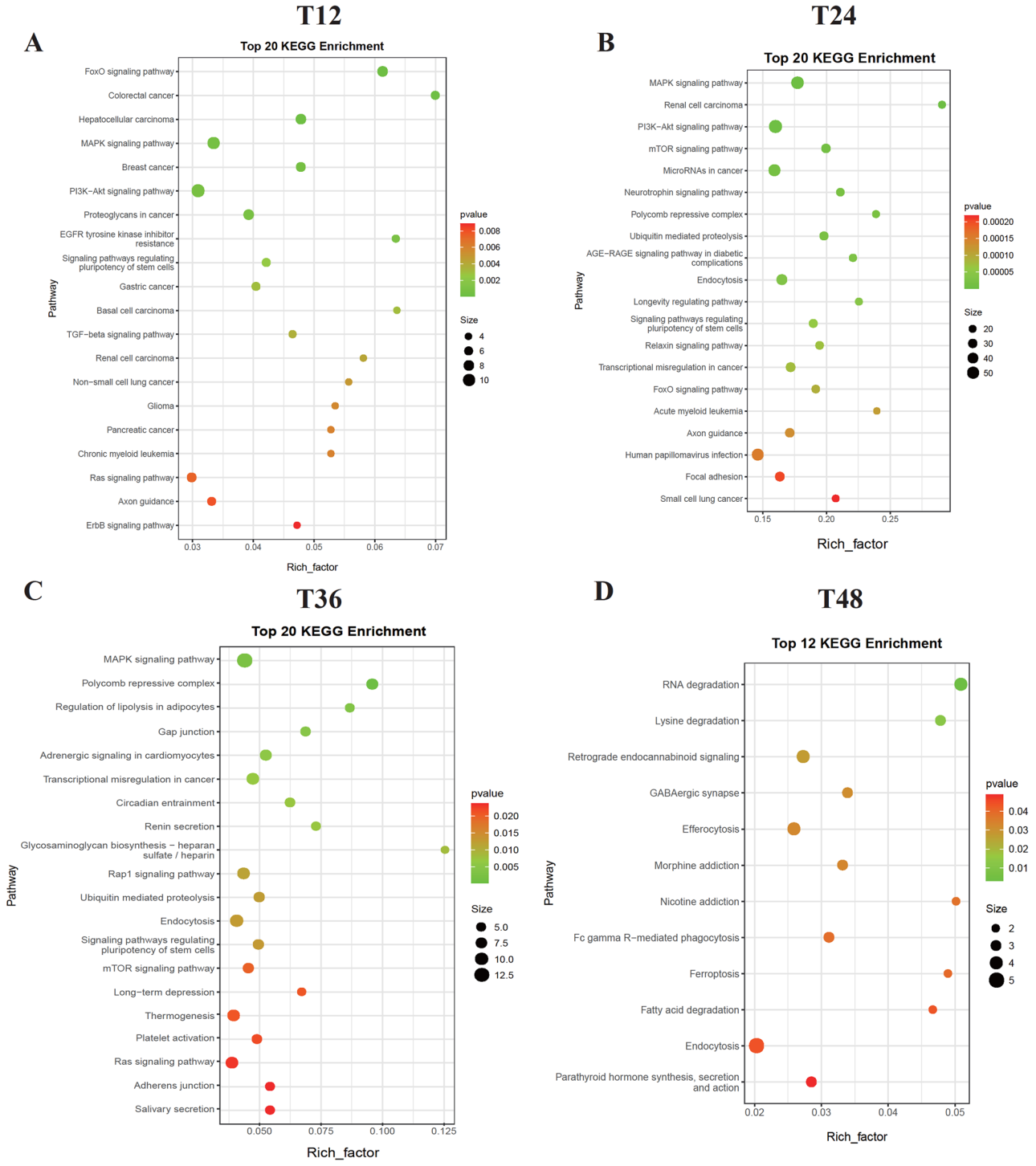

Fig. 4 Functional analyses for the target gene of specific miRNAs. (**A**), (**B**), (**C**) and (**D**) KEGG analyses for target genes of specific miRNAs in T12, T24, T36 and T48 groups. miRNA, microRNA; KEGG, Kyoto Encyclopedia of Genes and Genomes. The rich factor indicates the enrichment degree of terms, while vertical axis shows the names of the enriched terms. The area of the node represents the number of genes, and the *p*-value is shown by a color scale with the statistical significance increasing from green to red

(ID: hsa04010), "Renal cell carcinoma" (ID: hsa05211), "PI3K-Akt signaling pathway" (ID: hsa04151), "mTOR signaling pathway" (ID: hsa04150), "MicroRNAs in cancer" (ID: hsa05206), "Neurotrophin signaling pathway" (ID: hsa04722), "Relaxin signaling pathway" (ID: hsa04926), "Transcriptional misregulation in cancer" (ID: hsa05202), "FoxO signaling pathway" (ID: hsa04068), "Small cell lung cancer" (ID: hsa05222),

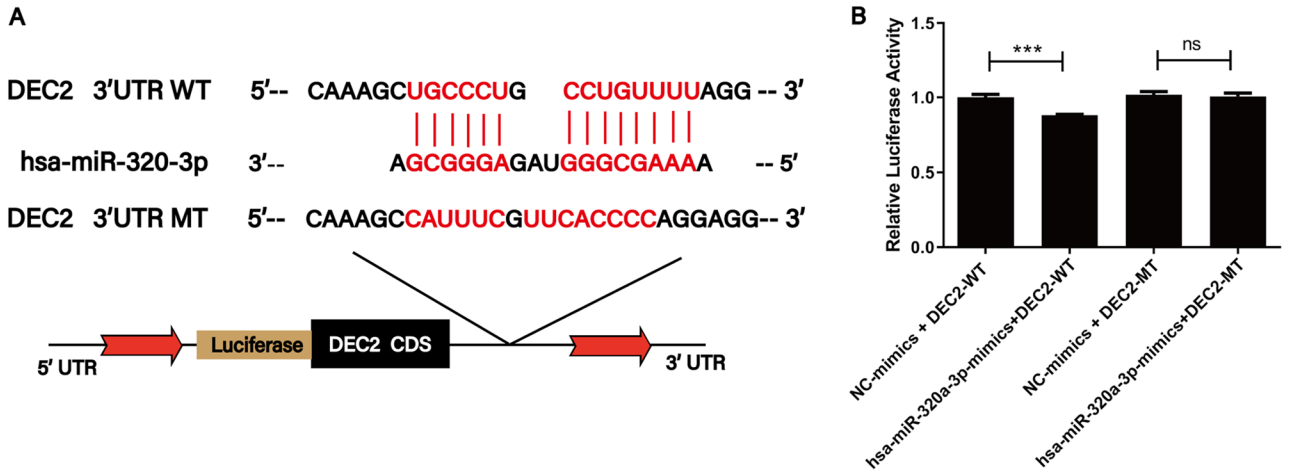

Fig. 5 The interaction between exsomal miR-320a-3p and its potential target gene (DEC2) was validated by the dual luciferase activity assay. DEC2, differentially expressed in chondrocytes protein 2; ***$P < 0.001$

"Proteoglycans in cancer" (ID: hsa05205), "TNF signaling pathway" (ID: hsa04668), "Colorectal cancer" (ID: hsa05210), "p53 signaling pathway" (ID: hsa04115), "Prostate cancer" (ID: hsa05215), "Ras signaling pathway" (ID: hsa04014), "Wnt signaling pathway" (ID: hsa04310), "Bladder cancer" (ID: hsa05219), "Non-small cell lung cancer"(hsa05223), "Endometrial cancer"(hsa05213), "TGF-beta signaling pathway"(hsa04350), "Rap1 signaling pathway"(hsa04015) and other related pathways. Moreover, the "Circadian rhythm" (ID: hsa04710) was also identified.

There were 314 putative target genes of the specific miRNAs in T36 group, and KEGG analyses indicated that 31 terms were identified ($P < 0.05$, FDR < 0.65) (Fig. 4C; Supplementary Table S6). Some enriched terms were associated with cancer and signaling, including "MAPK signaling pathway" (ID: hsa04010), "Adrenergic signaling in cardiomyocytes" (ID: hsa04261), "Transcriptional misregulation in cancer" (ID: hsa05202) "Renal cell carcinoma" (ID: hsa05211), "Ras signaling pathway" (ID: hsa04014) "mTOR signaling pathway" (ID: hsa04150) "Adherens junction" (ID: hsa04520) "Melanoma" (ID: hsa05218) and"Circadian entrainment" (ID: hsa04713).

There were 171 putative target genes of the specific miRNAs in T48 group, and the KEGG analyses were performed. The results indicated that 12 terms were enriched ($P < 0.05$, FDR < 0.65) (Fig. 4D; Supplementary Table S7), and most of these terms were associated with cancer and immune signaling, including "Retrograde endocannabinoid signaling" (ID: hsa04723), "Efferocytosis" (ID: hsa04148), "Fc gamma R-mediated phagocytosis" (ID: hsa04666) and "Ferroptosis" (ID: hsa04216).

Validation of the regulation between miRNAs and target gene

To further validate the prediction results of the miRNAs, a dual-luciferase assay was performed for verifying the regulative interaction between miR-320a-3p and its potential target gene (DEC2), which play key roles in regulating cell proliferation, apoptosis, circadian rhythm (CR) and epithelial-to-mesenchymal transition (EMT) of tumor cells [18]. The result showed that miR-320a-3p binding significantly reduced luciferase activity for the Wt target gene, whereas binding to the mutant site had no effect on luciferase activity (Fig. 5). Together, these results suggest that exosomal miRNAs have the potential regulating gene expression in cells.

Discussion

OC, the deadliest gynecological cancer, is the eighth most common cancer in women all over the world [19, 20]. Surgery, chemotherapy and immunotherapy are important treatments for OC, but the patients often succumb to recurrence for their limited therapeutic efficiency [21]. The tumor microenvironment (TME), which is composed of multiple different cellular and acellular components, can mediate tumor growth, invasion, metastasis and response to therapies [22]. Therefor, it is of importance to persistently explore the regulative mechanism associated with the TME of OC.

Exosomes, the double-membraned nanovesicles secreted by nearly all types of cells, are a subpopulation of the TME that transmit various biological molecules to promote intercellular communication [23]. In the current study, the exosomes were isolated successfully from the culture medium of OC cells (SKOV3) at the all time points, suggesting these cells could constantly secrete exosomes and regulate CM dynamically (Fig. 1B). Moreover, the morphology, dimension and average size of

exosomes from different groups were similar, suggesting that there might be steady intercellular communication and CM remodeling of OC cells.

Exosome contents not only reflect the composition of the donor cell but also indicate a regulated sorting mechanism [3, 24], and noncoding RNAs (ncRNAs) are among the most abundant contents in exosomes [25]. MicroRNAs (miRNAs), a type of regulatory ncRNA, are often incorporated into exosomes as signaling molecules and investigated intensely [9, 26]. In the current study, dynamic and regulative mechanisms of exosomal miRNAs was investigated by analyzing miRNAs expression of the exosomes which were collected at different time points (12, 24, 36, 48 h). A total of 131 miRNAs were identified, and there were only 15 common miRNAs, including seven let-7 family miRNAs (let-7a-5p, let-7b-5p, let-7c-5p, let-7e-5p, let-7f-5p, let-7 g-5p and let-7i-5p), suggesting that let-7 family microRNAs might play important roles in regulating CM of OC cells in exosome-mediated manner. In addition, 3, 57, 10 and 3 specific ones were found in T12, T24, T36 and T48 groups respectively, suggesting that regulative mechanism of exosomal miRNAs might changed dynamically. Interestingly, much more specific exosomal miRNAs were identified in T24 group, implying that the OC cells could package them into exsomes by a wonderful mechanism, which was deserved to be investigated in the future study.

Functional analyses revealed that both common and specific miRNAs have the capacities to regulate multiple genes associated with signaling and cancer (Figs. 3 and 4). Moreover, it indicated that exosomal miRNAs could regulate pathways associated with CR (Supplementary Table S4-S7). The CR is closely related to diseases [27], including OC [28, 29]. In the current study, the experiment of Western blotting indicated that expression levels of some circadian genes of OC cells, including *Clock*, *Bmal1*, *CRY1* and *Per2*, were obviously different at four time points (Figure S1), suggesting that exosomal miRNAs might play important roles in regulating CR of OC cells. In addition, the miR-320-3p was identified in the exosomes, and the experiments indicated this miRNA could mediate the DEC2 (Fig. 5). This suggests that we can further explore the relationship between this miRNAs and rhythm genes, as well as verify the regulation of this miRNA on disease and related signaling pathways in animal experiments.

Abbreviations

CM	Cellular microenvironment
OC	Ovarian cancer
miRNA-seq	miRNA sequencing
PBS	Phosphate buffer saline
TPM	Transcripts per million
GO	Gene Ontology
KEGG	Kyoto Encyclopedia of Genes and Genomes
RT	Reverse transcription
3' UTR	3′ untranslated region
Wt	Wild type
Mut	Mutant
mean ± SD	Mean ± standard deviation
FDR	False discovery rate
NCBI	National Center for Biotechnology Information
CR	Circadian rhythm
EMT	Epithelial-to-mesenchymal transition
TME	Tumor microenvironment
ncRNAs	Noncoding RNAs
miRNAs	MicroRNAs

Supplementary Information

The online version contains supplementary material available at https://doi.org/10.1186/s13048-025-01608-3.

Supplementary Material 1: Western blot analysis of differential expression of circadian genes in ovarian cancer cells at four time points

Supplementary Material 2: The list of identified miRNAs.

Supplementary Material 3: GO analyses of overlapping miRNA target genes in T12, T24, T36 and T48 groups.

Supplementary Material 4: KEGG analyses of overlapping miRNA target genes in T12, T24, T36 and T48 groups.

Supplementary Material 5: KEGG analysis for target genes of specific miRNAs in T12 group.

Supplementary Material 6: KEGG analysis for target genes of specific miRNAs in T24 group.

Supplementary Material 7: KEGG analysis for target genes of specific miRNAs in T36 group.

Supplementary Material 8: KEGG analysis for target genes of specific miRNAs in T48 group.

Acknowledgements
We thank members of Wuhan GeneCreate Biological Engineering Limited for discussions, and in particular Dr. Leilei Zhan for critical reading of the manuscript.

Author contributions
ZW: Investigation, Methodology, Project administration, Resources, Software, Visualization, Writing-original draft, Writing-review& editing. YH: Conceptualization, Data curation, Investigation, Project administration, Writing–original draft. SH: Formal analysis, Resources, Software, Supervision, Validation, Visualization, Writing- original draft, Writing–review& editing.YZ: Writing–review& editing, Validation. LZ: Writing -review& editing, Validation. FW: Writing–review& editing, Validation.

Funding
This work was supported by the Key Medical Research Projects of Shanxi Province (***2021XM36***).

Data availability
The datasets generated in the current study were deposited in the National Center for Biotechnology Information (NCBI) under the accession number PRJNA1108066. All data analyzed in this study are shown in the supplementary table and supplementary figures.

Declarations

Ethics approval and consent to participate
Not applicable.

Consent for publication
Not applicable.

Informed consent statement
Not applicable.

Competing interests
The authors declare no competing interests.

Received: 3 June 2024 / Accepted: 23 January 2025
Published online: 10 February 2025

References

1. Xu Z, Chen Y, Ma L, Chen Y, Liu J, Guo Y, et al. Role of exosomal non-coding RNAs from tumor cells and tumor-associated macrophages in the tumor microenvironment. Mol Ther. 2022;30(10):3133–54.
2. Joshi BS, de Beer MA, Giepmans BN, Zuhorn IS. Endocytosis of extracellular vesicles and release of their cargo from endosomes. ACS Nano. 2020;14(4):4444–55.
3. Kalluri R, LeBleu VS. The biology, function, and biomedical applications of exosomes. Science. 2020;367(6478):eaau6977.
4. Malla RR, Shailender G, Kamal MA. Exosomes: critical mediators of tumour microenvironment reprogramming. Curr Med Chem. 2021;28(39):8182–202.
5. Paskeh MDA, Entezari M, Mirzaei S, Zabolian A, Saleki H, Naghdi MJ, et al. Emerging role of exosomes in cancer progression and tumor microenvironment remodeling. J Hematol Oncol. 2022;15(1):83.
6. Chang W-H, Cerione RA, Antonyak MA. Extracellular vesicles and their roles in cancer progression. Cancer cell Signaling: Methods Protocols. 2021:143–70.
7. Han Q-F, Li W-J, Hu K-S, Gao J, Zhai W-L, Yang J-H, et al. Exosome biogenesis: machinery, regulation, and therapeutic implications in cancer. Mol Cancer. 2022;21(1):207.
8. Latifkar A, Hur YH, Sanchez JC, Cerione RA, Antonyak MA. New insights into extracellular vesicle biogenesis and function. J Cell Sci. 2019;132(13):jcs222406.
9. Liu M, Yu X, Bu J, Xiao Q, Ma S, Chen N, et al. Comparative analyses of salivary exosomal miRNAs for patients with or without lung cancer. Front Genet. 2023;14:1249678.
10. Langmead B, Trapnell C, Pop M, Salzberg SL. Ultrafast and memory-efficient alignment of short DNA sequences to the human genome. Genome Biol. 2009;10:1–10.
11. Kozomara A, Griffiths-Jones S. miRBase: annotating high confidence microRNAs using deep sequencing data. Nucleic Acids Res. 2014;42(D1):D68–73.
12. Krek A, Grün D, Poy MN, Wolf R, Rosenberg L, Epstein EJ, et al. Combinatorial microRNA target predictions. Nat Genet. 2005;37(5):495–500.
13. Lewis BP, Burge CB, Bartel DP. Conserved seed pairing, often flanked by adenosines, indicates that thousands of human genes are microRNA targets. Cell. 2005;120(1):15–20.
14. Huang DW, Sherman BT, Lempicki RA. Systematic and integrative analysis of large gene lists using DAVID bioinformatics resources. Nat Protoc. 2009;4(1):44–57.
15. Livak KJ, Schmittgen TD. Analysis of relative gene expression data using real-time quantitative PCR and the 2 – ΔΔCT method. Methods. 2001;25(4):402–8.
16. Li C, Zhou T, Chen J, Li R, Chen H, Luo S, et al. The role of Exosomal miRNAs in cancer. J Translational Med. 2022;20:1–15.
17. Zou X, Huang Z, Guan C, Shi W, Gao J, Wang J et al. Exosomal miRNAs in the microenvironment of pancreatic cancer. Clin Chim Acta. 2023:117360.
18. Sato F, Bhawal UK, Yoshimura T, Muragaki Y. DEC1 and DEC2 crosstalk between circadian rhythm and tumor progression. J Cancer. 2016;7(2):153.
19. Wang Z, Li F, Wei M, Zhang S, Wang T. Circadian clock protein PERIOD2 suppresses the PI3K/Akt pathway and promotes cisplatin sensitivity in ovarian cancer. Cancer Manage Res. 2020:11897–908.
20. Zhang R, Siu MK, Ngan HY, Chan KK. Molecular biomarkers for the early detection of ovarian cancer. Int J Mol Sci. 2022;23(19):12041.
21. Yang C, Xia B-R, Zhang Z-C, Zhang Y-J, Lou G, Jin W-L. Immunotherapy for ovarian cancer: adjuvant, combination, and neoadjuvant. Front Immunol. 2020;11:577869.
22. Elhanani O, Ben-Uri R, Keren L. Spatial profiling technologies illuminate the tumor microenvironment. Cancer Cell. 2023;41(3):404–20.
23. Jin Y, Xing J, Xu K, Liu D, Zhuo Y. Exosomes in the tumor microenvironment: promoting cancer progression. Front Immunol. 2022;13:1025218.
24. Isaac R, Reis FCG, Ying W, Olefsky JM. Exosomes as mediators of intercellular crosstalk in metabolism. Cell Metabol. 2021;33(9):1744–62.
25. Tang X-H, Guo T, Gao X-Y, Wu X-L, Xing X-F, Ji J-F, et al. Exosome-derived noncoding RNAs in gastric cancer: functions and clinical applications. Mol Cancer. 2021;20:1–15.
26. Garcia-Martin R, Wang G, Brandão BB, Zanotto TM, Shah S, Kumar Patel S, et al. MicroRNA sequence codes for small extracellular vesicle release and cellular retention. Nature. 2022;601(7893):446–51.
27. Neves AR, Albuquerque T, Quintela T, Costa D. Circadian rhythm and disease: relationship, new insights, and future perspectives. J Cell Physiol. 2022;237(8):3239–56.
28. Wang Z, Li F, He S, Zhao L, Wang F. Period circadian regulator 2 suppresses drug resistance to cisplatin by PI3K/AKT pathway and improves chronochemotherapeutic efficacy in cervical cancer. Gene. 2022;809:146003.
29. Zhu J, Zhou Q, Pan M, Zhou C. Multi-omics analysis of the prognosis and therapeutic significance of circadian clock in ovarian cancer. Gene. 2021;788:145644.

Publisher's note